Journal of
Mechanics of
Materials and Structures

A SEMIANALYTICAL SOLUTION FOR FREE VIBRATION ANALYSIS OF STIFFENED CYLINDRICAL SHELLS

Guanghui Qing, Zhenyu Feng, Yanhong Liu
and Jiaujun Qiu

Volume 1, Nº 1 January 2006

mathematical sciences publishers

JOURNAL OF MECHANICS OF MATERIALS AND STRUCTURES
Vol. 1, No. 1, 2006

A SEMIANALYTICAL SOLUTION FOR FREE VIBRATION ANALYSIS OF STIFFENED CYLINDRICAL SHELLS

GUANGHUI QING, ZHENYU FENG, YANHONG LIU AND JIAUJUN QIU

Based on a semianalytical solution of the state-vector equations, we propose a novel mathematical model for the free vibration analysis of cylindrical shells with stiffeners and for cylindrical panels with discontinuities in thickness and/or with cutouts. The shell and stiffeners are regarded as three-dimensional elastic bodies, but the same quadrilateral element is used to discretize the shell and stiffeners. The method accounts for the compatibility of displacements and stresses on the interface between layers of the laminated shell and stiffeners, for transverse shear deformation, and of course for the rotational inertia of the shell and stiffeners. To demonstrate the model's excellent predictive abilities, several examples are analyzed numerically.

The model can be easily modified to solve problems of stiffened piezolaminated plates and shells, or plates and shells with patches made of a piezoelectric material.

1. Introduction

A sheet-stiffener combination provides the maximum strength-to-weight ratio for any structure and hence becomes the obvious choice in advanced structures such as pressure vessels, airplanes, submarine hells and missiles. These structures are subject to external dynamic loads. Therefore, prediction of dynamic responses is of considerable interest for engineers.

Stiffened shells or plates can be analyzed by considering equivalent orthotropic systems. This method is mainly applicable only when large numbers of stiffeners are closely and evenly spaced. Another method, treating separately the shell/plate and stiffeners, is more general as it can accommodate any stiffener distribution.

For ring-stiffened or string-stiffened circular cylindrical shells there have been many investigations involving free vibration analysis or dynamic response analysis. Al-Najafi and Warburton [1970], using the finite element method, investigated the

Keywords: free vibration, stiffened cylindrical shells, laminated cylindrical shells, semianalytical solution, state-vector equation.

Work supported by Scientific Research Initiation Foundation of CAUC (Grant No. 05QD01S) and the National Natural Science Foundation of China (Grant No. 10072038).

.

natural frequencies and mode shapes of thin circular cylindrical shells with stiffening rings. Wilken and Soedel [1976] employed the receptance method to determine the natural frequencies and mode shapes of circular cylindrical shells stiffened by rings. Stanley and Ganessan [1997] used circular cylindrical shell elements and studied the natural frequencies of stiffened cylindrical shells for short and long shells with clamped-clamped boundary condition. Zhao, Liew, and Ng [Zhao et al. 2002], using an energy approach, investigated the free vibration of stiffened simply supported rotating cross-ply laminated cylindrical shells. Gong and Lam [1998], using layered shell elements for both plate and stiffener in MSC/Patran and LS-DYNA3D, carried out a transient response analysis of a stiffened composite submersible hull. Rikards, Chate, and Ozolinsh [Rikards et al. 2001] developed a triangular finite element method for the study of the free vibrations of stiffened laminated composite shells. Yang and Zhou [1995] used the transfer function method to analyze the free vibration of a ring-stiffened shell. Wang, Swaddiwudhipong and Tian [Wang et al. 1997] investigated the free vibration problem for isotropic cylindrical shells with varying ring-stiffener distribution, using the extended Ritz method. Kim and Lee [2002] analyzed the effects of ring stiffeners on vibration characteristics and transient responses for ring-stiffened composite cylindrical shells subject to step pulse loading. Srinivasan and Krishnan [1989] studied the dynamic response analysis of stiffened conical shell panels. Sinha and Mukhopadhyay [1995] investigated the dynamic response of stiffened plates and shells by the finite element method employing a high-precision arbitrary-shaped triangular shell element in which stiffeners may lie in arbitrary directions within the element. Liao and R. [1994] studied the dynamic stability of laminated composite stiffened or nonstiffened plates and shells due to periodic in-plane forces at boundaries using the finite element method.

The semianalytical method is an important approach in the analysis of multilayered structures with complicated boundary conditions [Zou and Tang 1995b; 1995a; Sheng and Ye 2002b; 2002a; 2003]. The main theory used in these references is state-vector equation theory. Based on the mixed formulation of solid mechanics, we use the finite element approach in the plane and once the transfer matrix of a single layer is obtained, we introduce interface continuity conditions to assemble a global matrix of structures. The advantages of this semianalytical solution method are:

1. The order of the global matrix does not depend on the number of layers, since the matrix is obtained by the multiplication of the transfer matrix of each layer via an interface continuity condition. Hence the three-dimensional problem is transformed into a two-dimensional one.

2. "The varying material and geometric properties along the independent spatial variable are allowed" [Steele and Kim 1992].

3. Anisotropic layered materials can be simply handled [Steele and Kim 1992].

In this paper, a general, novel semianalytical solution for the free vibration analysis of cylindrical shells with different stiffeners and cylindrical panels with discontinuity in the thickness or/and with cutouts is achieved through the separate consideration of the shell and stiffeners. On the basis of the state-vector equation theory, the quadrilateral elemental equation is written in a matrix differential equation of the first order, and the global algebraic equation of the shell and stiffeners are established separately. Transverse shear deformation and rotational inertia are also considered in the model. In Section 3 several numerical examples are analyzed, and the convergence of some of examples is tested.

2. The formulas of the thin shells and stiffened laminated shell

Some typical stiffened circular cylindrical shells are shown in Figures 1–4.

The shells shown in Figures 1 and 2 are commonly called stiffened shells with ring or/and string stiffeners. Those in Figures 3 and 4 are generally called shells with discontinuity in thickness. In fact, all can be regarded as shells with different stiffeners. For example, a laminated shell with discontinuity in thickness, like that of Figure 3, is made up of a laminated circular cylindrical shell and a laminated stiffener, as shown in Figure 5.

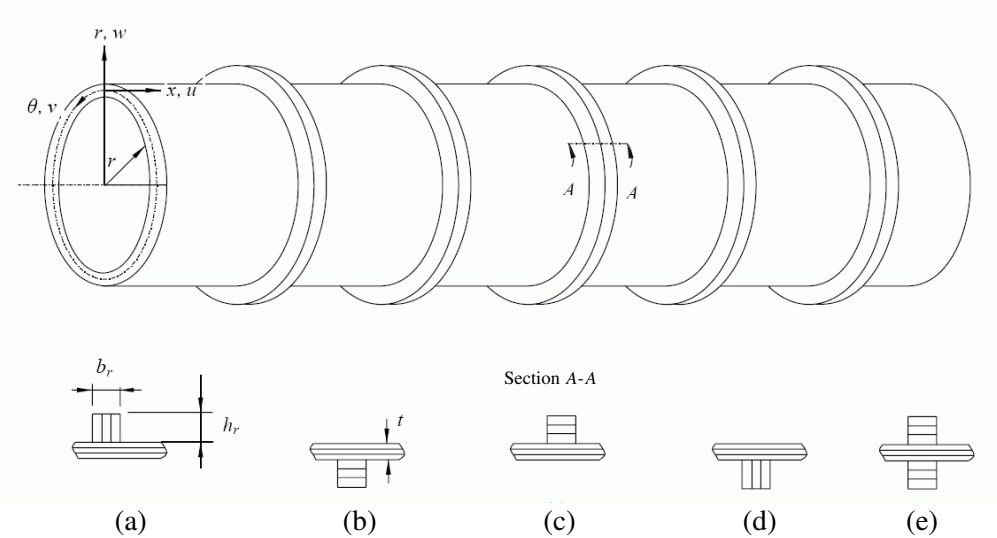

Figure 1. A laminated shell with ring stiffeners: (a) external type 2; (b) internal type 1; (c) external type 1; (d) internal type 2; and (e) concentric type 1.

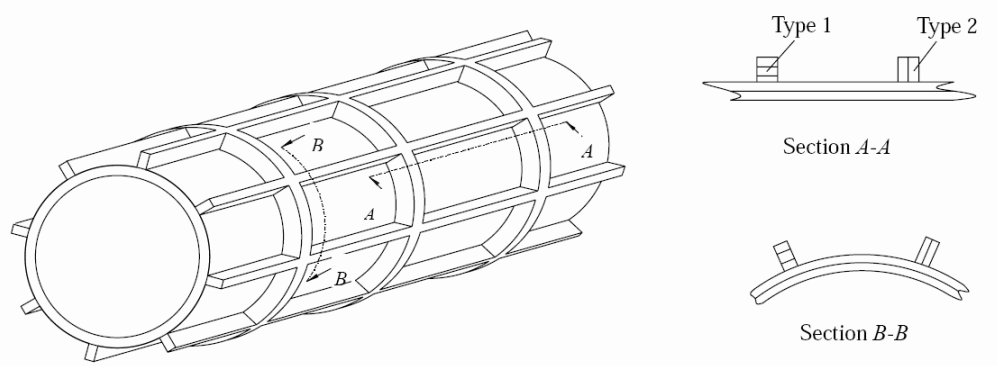

Figure 2. A laminated shell with three rings and eight string stiffeners.

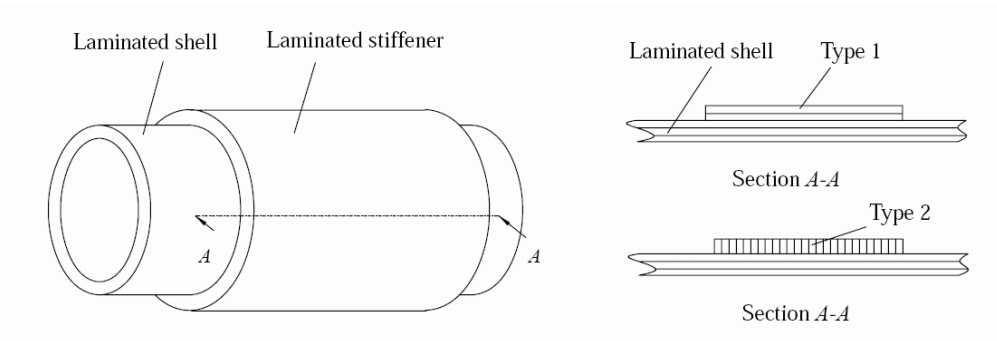

Figure 3. A laminated shell with discontinuity in thickness (one ring stiffener).

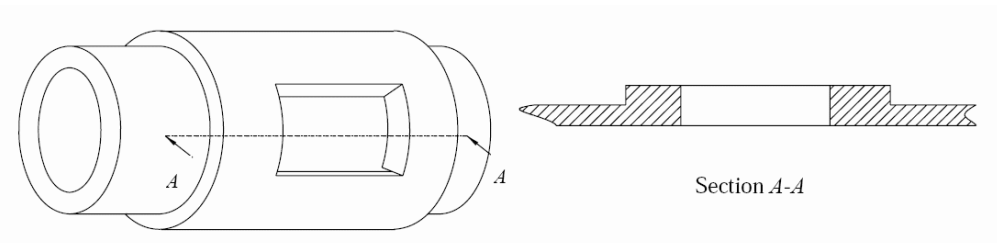

Figure 4. A circular cylindrical shell with a cutout and discontinuity in thickness.

Our laminated shells are considered as n-layered shells (see Figure 1 for the coordinate system). Assuming the material of an arbitrary layer has orthotropic

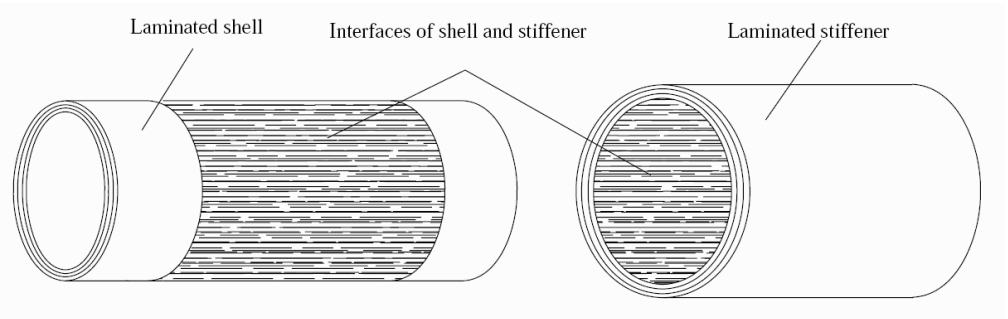

Figure 5. Decomposition of a shell with discontinuity in thickness.

symmetry with respect to the coordinate planes, the stress-displacement relationships can be stated as

$$\begin{pmatrix} \sigma_x \\ \sigma_\theta \\ \sigma_r \\ \tau_{\theta r} \\ \tau_{xr} \\ \tau_{x\theta} \end{pmatrix} = \begin{bmatrix} C_{11} & C_{12} & C_{13} & 0 & 0 & 0 \\ & C_{22} & C_{23} & 0 & 0 & 0 \\ & & C_{33} & 0 & 0 & 0 \\ & & & C_{44} & 0 & 0 \\ & \text{(symm.)} & & & C_{55} & 0 \\ & & & & & C_{66} \end{bmatrix} \begin{pmatrix} \alpha u \\ \beta v/r + w/r \\ \partial w/\partial r \\ \beta w/r + \partial v/\partial r - v/r \\ \alpha w + \partial u/\partial r \\ \beta u/r + \alpha v \end{pmatrix}$$

where σ_x, σ_θ, σ_r, $\tau_{\theta r}$, tau_{xr}, and $\tau_{x\theta}$ are the stress components, the C_{ij} $(i, j = 1, 2, \ldots, 6)$ denote the elasticity coefficient of the material, $\alpha = \partial/\partial x$, $\beta = \partial/\partial\theta$, and u, v, w are the displacements in the x, θ and r directions, respectively.

The modified mixed H-R variational principle [Zou and Tang 1995b; 1995a; Steele and Kim 1992] can be expressed as

$$\delta \prod = \delta\left(\iiint_V (\boldsymbol{p}^T \cdot \dot{\boldsymbol{q}} - H)\, r\, dx\, d\theta\, dr - \iint_{S_\sigma} \boldsymbol{q}^T \cdot (\boldsymbol{T} - \overline{\boldsymbol{T}})\, ds_\sigma - \iint_{S_u} \boldsymbol{T}^T \cdot (\boldsymbol{q} - \bar{\boldsymbol{q}})\, ds_u \right), \quad (1)$$

where $\boldsymbol{q} = [u \;\; v \;\; w]^T$, $\boldsymbol{p} = [\tau_{xr} \;\; \tau_{\theta r} \;\; \sigma_r]^T$, $\dot{\boldsymbol{q}} = \partial \boldsymbol{q}/\partial r$, $\boldsymbol{T} = [T_x \;\; T_\theta \;\; T_r]^T$, $\overline{\boldsymbol{T}} = [\overline{T}_x \;\; \overline{T}_\theta \;\; \overline{T}_r]^T$ represents the stresses acting on the stress boundaries S_σ, and $\bar{\boldsymbol{q}} = [\bar{u} \;\; \bar{v} \;\; \bar{w}]^T$ represents the displacements on the displacement boundaries S_u. The Hamiltonian H can be written (neglecting the body force) as

$$\begin{aligned} -H = {} & \left(C_3\alpha u + C_4(r^{-1}\beta v + r^{-1}w) - C_5\sigma_r\right)(r^{-1}\beta v + r^{-1}w) \\ & + \left(C_2\alpha u + C_3(r^{-1}\beta v + r^{-1}w) - C_1\sigma_r\right)\alpha u + C_6(r^{-1}\alpha v + r^{-1}u)(\alpha v + r^{-1}\beta u) \\ & + \tau_{\theta r}(r^{-1}\beta w - r^{-1}v) + \tau_{xr}\alpha w - 2^{-1}\boldsymbol{\eta}^T\boldsymbol{S}\boldsymbol{\eta} - 2^{-1}\rho(\omega^2u^2 + \omega^2v^2 + \omega^2w^2), \end{aligned}$$

Figure 6. The local coordinate system of a quadrilateral element.

where

$$\boldsymbol{\eta} = \begin{pmatrix} C_2\alpha u + C_3(r^{-1}\beta v + r^{-1}w) - C_1\sigma_r \\ C_3\alpha u + C_4(r^{-1}\beta v + r^{-1}w) - C_5\sigma_r \\ \sigma_r\ \tau_{\theta r}\ \tau_{xr}\ C_6(\alpha v + r^{-1}\beta u) \end{pmatrix},$$

ρ is the mass density, ω is the natural frequency, and

$$\begin{aligned} C_1 &= -C_{13}/C_{33}, & C_4 &= C_{22} - C_{23}^2/C_{33}, & C_7 &= 1/C_{33}, \\ C_2 &= C_{11} - C_{13}^2/C_{33}, & C_5 &= -C_{23}/C_{33}, & C_8 &= 1/C_{55}, \\ C_3 &= C_{12} - C_{13}C_{23}/C_{33}, & C_6 &= C_{66}, & C_9 &= 1/C_{44}. \end{aligned}$$

Using a quadrilateral element with local coordinate system as in Figure 6, the field functions and the shape functions assume the form

$$\begin{gathered} u = [\boldsymbol{N}(x,\theta)]\big(u(r)\big), \qquad v = [\boldsymbol{N}(x,\theta)]\big(v(r)\big), \qquad w = [\boldsymbol{N}(x,\theta)]\big(w(r)\big), \\ \tau_{\theta r} = [\boldsymbol{N}(x,\theta)]\big(\tau_{\theta r}(r)\big), \quad \tau_{xr} = [\boldsymbol{N}(x,\theta)]\big(\tau_{xr}(r)\big), \quad \sigma_r = [\boldsymbol{N}(x,\theta)]\big(\sigma_r(r)\big), \quad (2) \\ N_i(\xi,\eta) = \tfrac{1}{4}(1+\xi_i\xi)(1+\eta_i\eta) \quad \text{for } i = 1,2,3,4, \end{gathered}$$

The x-θ curved surface of a layer is discretized as shown in Figure 7.

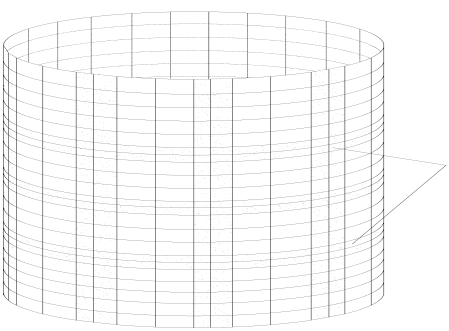

Figure 7. The element meshes of an arbitrary layer of a laminated shell.

Assume the stress boundaries are satisfied ($\boldsymbol{T} = \overline{\boldsymbol{T}}$), and the displacement boundaries of arbitrary layer are satisfied ($\boldsymbol{q} = \bar{\boldsymbol{q}}$). Substituting Equations (2) into (1) and using $\delta \prod = 0$ we obtain the element state-vector equation

$$\boldsymbol{C}^e \frac{d\boldsymbol{H}^e(r)}{dr} = \boldsymbol{K}^e \boldsymbol{H}^e(r). \tag{3}$$

The detailed forms of $\boldsymbol{C}^e$, $\boldsymbol{K}^e$ and $\boldsymbol{H}^e(r)$ in (3) can be found in the Appendix.

The detailed treatments on the various boundary conditions can be found in [Sheng and Ye 2002b].

The standard finite element assemblage process is used. The global state-vector equation for m-th layer takes the form

$$\boldsymbol{C}_m \frac{d\boldsymbol{H}_m(r)}{dr} = \boldsymbol{K}_m \boldsymbol{H}_m(r), \tag{4}$$

with general solution

$$\boldsymbol{H}_m(r_{i,m}) = \boldsymbol{T}_m(h_m)\boldsymbol{H}_m(r_{o,m}), \tag{5}$$

where $\boldsymbol{T}_m(h_m) = e^{\boldsymbol{C}_m \boldsymbol{K}_m \cdot (h_m)}$, $h_m$is the thickness of m-th layer and $h_m = r_{i,m} - r_{o,m}$ is the difference between the inside and outside radii of the m-th layer. When we compute $e^{\boldsymbol{C}_m \boldsymbol{K}_m \cdot h_m}$, the r of each layer in $\boldsymbol{K}_m$ is replaced by $r = (r_{o,m} - r_{i,m})/2$.

The exponential of a matrix can be computed in many ways (approximation theory, differential equations, eigenvalues, characteristic polynomial, and so on). In practice, considerations of stability, efficiency and accuracy make some methods preferable to others, but none is completely satisfactory [Moler and Van Loan 1978]. Hence, the precise integration method [Zhong and Zhu 1996; Zhong 2001] for Equation (4) is employed for the calculations in this paper.

Equation (5) must be satisfied at every layer of our n-layered shell. Based on the compatibility conditions for the displacements and stresses at the interface between two layers, we obtain the recursive formulation

$$\boldsymbol{H}_n(r_{i,n}) = \Big(\prod_{m=1}^{n} \boldsymbol{T}_m \Big) \boldsymbol{H}_1(r_{o,1}), \tag{6}$$

in which $r_{i,n}$, $r_{o,1}$ are the inner and outer radii of the n-layered shell.

Equation (6) expresses the relationship between the physical quantities for the external and internal surface of an n-layered shell. It amounts to a set of linear algebraic equations in terms of node displacements and stresses. In matrix form, this can be written as

$$\begin{pmatrix} \boldsymbol{q}_n(r^s_{i,n}) \\ \boldsymbol{p}_n(r^s_{i,n}) \end{pmatrix} = \begin{bmatrix} \boldsymbol{T}^s_{11} & \boldsymbol{T}^s_{12} \\ \boldsymbol{T}^s_{21} & \boldsymbol{T}^s_{22} \end{bmatrix} \begin{pmatrix} \boldsymbol{q}_1(r^s_{o,1}) \\ \boldsymbol{p}_1(r^s_{o,1}) \end{pmatrix} \tag{7}$$

where the superscript s denotes the laminated shell.

A laminated stiffener is also considered as an l-layered shell, and the element mesh in every layer is assumed to be the same (shaded part of Figure 7). The procedure above for the external and internal stiffeners is repeated, and yields the equations

$$\begin{pmatrix} \boldsymbol{q}_l(r_{i,l}^{es}) \\ \boldsymbol{p}_l(r_{i,l}^{es}) \end{pmatrix} = \begin{bmatrix} \boldsymbol{T}_{11}^{es} & \boldsymbol{T}_{12}^{es} \\ \boldsymbol{T}_{21}^{es} & \boldsymbol{T}_{22}^{es} \end{bmatrix} \begin{pmatrix} \boldsymbol{q}_1(r_{o,1}^{es}) \\ \boldsymbol{p}_1(r_{o,1}^{es}) \end{pmatrix} \tag{8}$$

$$\begin{pmatrix} \boldsymbol{q}_l(r_{i,l}^{is}) \\ \boldsymbol{p}_l(r_{i,l}^{is}) \end{pmatrix} = \begin{bmatrix} \boldsymbol{T}_{11}^{is} & \boldsymbol{T}_{12}^{is} \\ \boldsymbol{T}_{21}^{is} & \boldsymbol{T}_{22}^{is} \end{bmatrix} \begin{pmatrix} \boldsymbol{q}_1(r_{o,1}^{is}) \\ \boldsymbol{p}_1(r_{o,1}^{is}) \end{pmatrix} \tag{9}$$

where superscript *es* and *is* denote the external and internal stiffeners, and $r_{i,l}^{es}$, $r_{i,l}^{is}$, $r_{o,1}^{es}$, $r_{o,1}^{is}$ are the inside and outer radius of the external and internal stiffeners.

Noted that the dimensionality of (8) and (9) differs from that of (7).

The displacements and stresses on the interface between shell and stiffeners must be continuous. Uniting (7), (8) and (9) yields

$$\begin{pmatrix} \boldsymbol{q}(r_i) \\ \boldsymbol{p}(r_i) \end{pmatrix} = \begin{bmatrix} \boldsymbol{T}_{11} & \boldsymbol{T}_{12} \\ \boldsymbol{T}_{21} & \boldsymbol{T}_{22} \end{bmatrix} \begin{pmatrix} \boldsymbol{q}(r_o) \\ \boldsymbol{p}(r_o) \end{pmatrix}. \tag{10}$$

We can see that the node number of a layer of a laminated shell determines the number of variables in (10); thus this number of variables has no relationship to the thickness of the shell or the height and number of stiffeners.

Because we are studying natural frequencies, so the external surface and internal surface are traction-free (the stress column vector $\boldsymbol{p}(r_i)$ and $\boldsymbol{p}(r_o)$ are zero), we deduce from (10) that

$$\boldsymbol{T}_{21}\boldsymbol{q}(r_o) = 0.$$

For this to have nontrivial solutions, the determinant of the characteristic matrix must be zero:

$$|\boldsymbol{T}_{21}| = 0.$$

The natural frequencies ω can be obtained from the characteristic polynomial of this last equation through the use of the bisection method [Johnston 1982]. To simplify the analysis and improve the accuracy of the results, dimensionless versions of u, v, w, τ_{xr}, $\tau_{\theta r}$, and σ_r need to be used in the computer program.

3. Numerical examples and discussions

Example 1. As a first test of our method we discuss an example studied experimentally and theoretically by Al-Najafi and Warburton [1970], consisting of a stiffened external steel shell with five identical ring stiffeners (Figure 1). The dimensions of the shell are: inside diameter $d = 0.2158$ m; length $l = 0.4572$ m; thickness $t = 0.00386$ m; breadth of rings $b_r = 0.00635$ m; height of rings $h_r = 0.00635$ m,

0.01778m , 0.0254 m. There are six bays of equal length. Material properties: Young's modulus $E = 204.0\,\text{GPa}$; shear modulus $G = 79.0\,\text{GPa}$; density $\rho = 7840\,\text{kg m}^{-3}$.

Because compatible finite elements in the x-θ plane are used, the natural frequencies should converge the the values of the mathematical model monotonically as the number of elements in the discretization is increased. The results, listed in Table 1, show that reasonable convergence has been achieved with relatively small

Mesh : layers ($k \times m : n$)		Mode number							
		F-F (Free ends)				S-S (Simply supported ends)			
Shell	Stiffeners	1	2	3	4	1	2	3	4
$h_r = 0.00635\,\text{m}$									
23×36:1	1×36:1	322.2	338.3	889.5	948.2	840.5	1103.2	1734.7	1808.5
35×45:1	1×45:1	317.2	333.5	867.2	925.5	834.2	1089.6	1719.0	1789.8
47×60:1	2×60:2	314.6	331.9	859.1	920.0	831.8	1074.3	1697.0	1780.7
58×72:1	2×72:2	313.2	330.8	856.4	918.4	831.1	1069.7	1694.9	1776.3
		(2,2)	(2,1)	(3,2)	(3,1)	(2,1)	(3,1)	(3,2)	(0,1)
Experimental		323	342	865	928	809	1065	1658	/
Finite element		317	340	861	926	834	1065	1699	/
$h_r = 0.01778\,\text{m}$									
23×36:1	1×36:2	636.6	752.9	1506.3	1533.3	1030.9	1640.2	2096.5	2340.7
35×45:1	1×45:3	621.7	733.4	1474.0	1502.9	1017.1	1625.4	2073.4	2313.3
47×60:1	2×60:4	618.9	726.1	1450.5	1480.7	1012.2	1608.9	2040.2	2292.1
58×72:1	2×72:4	618.5	723.4	1443.0	1464.1	1011.4	1602.9	2055.3	2284.2
		(2,2)	(2,1)	(3,2)	(3,1)	(2,1)	(0,1)	(3,1)	(2,2)
Experimental		626	743	1437	1468	996	/	2017	2277
Finite element		626	746	1438	1465	1031	/	2060	2390
$h_r = 0.0254\,\text{m}$									
23×36:1	1×36:3	830.9	1002.7	1705.0	1703.2	1214.2	1491.4	2296.6	2601.8
35×45:1	1×45:4	815.5	974.7	1677.1	1672.7	1193.1	1485.4	2273.6	2582.7
47×60:1	2×60:5	806.4	963.6	1640.8	1645.4	1191.2	1482.3	2264.2	2564.5
58×72:1	2×72:5	803.5	971.0	1634.9	1639.2	1189.5	1481.3	2259.4	2546.7
		(2,2)	(2,1)	(3,1)	(3,2)	(2,1)	(0,1)	(2,2)	(3,1)
Experimental		814	982	1627	1632	1187	/	2082	2522
Finite element		822	997	1629	1636	1223	/	2279	2607

Table 1. Convergence of natural frequencies (Hz) for steel external shell with 5 ring stiffeners (Example 1). Rows "Experimental" and "Finite element" are from [Al-Najafi and Warburton 1970].

decrements in the four frequencies, never as much as 1%, between corresponding values for the 47×60 and 58×72 meshes (both one layer).

Figure 8 gives the four mode shapes for Example 1 with simply supported ends. We see that the effect of the stiffening rings on the mode shape increases as h_r increases.

Example 2. In this example (Figure 9) the shell has two identical face layers with thicknesses t_e and t_i, and a core layer of thickness t_c. All three layers have the material properties corresponding to aragonite crystals, which have stiffness ratios

$$\begin{aligned} C_{22}/C_{11} &= 0.543103, & C_{12}/C_{11} &= 0.23319, \\ C_{23}/C_{11} &= 0.098276, & C_{44}/C_{11} &= 0.26681, \\ C_{33}/C_{11} &= 0.530172, & C_{55}/C_{11} &= 0.159914, \\ C_{13}/C_{11} &= 0.010776, & C_{66}/C_{11} &= 0.262931. \end{aligned}$$

We assume $C_{11} = 150\,\text{GPa}$ and $\rho = 1600\,\text{kg/m}^3$ for the two face layers and $C_{11} = 75\,\text{GPa}$ and $\rho = 800\,\text{kg/m}^3$ for the core layer of the laminated shell. We take the material properties of stiffeners to be the same as those of the face layers. The convergence of the first four natural frequencies is listed in Table 2.

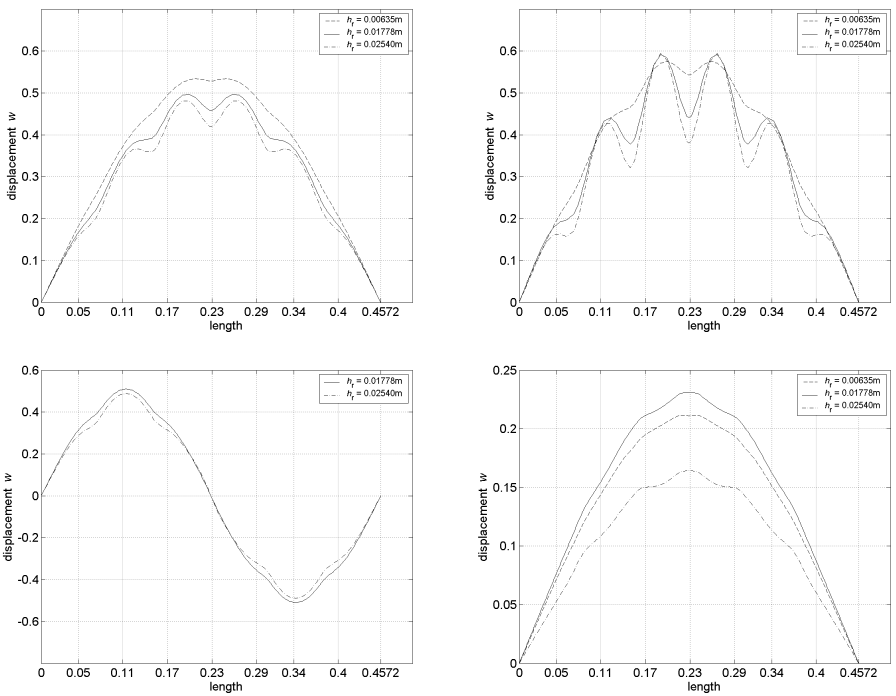

Figure 8. Four mode shapes for Example 1. Clockwise from top left: (2, 1), (3, 1), (0, 1), (2, 2).

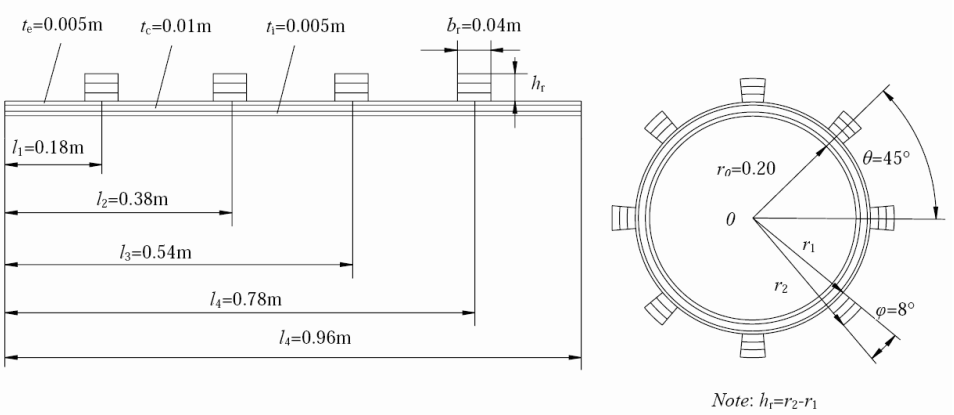

Figure 9. Dimensions of stiffened laminated shell with ring and string stiffeners (Example 2).

Mesh : layers ($k \times m : n$)			Mode number			
Shell	Rings	Strings	1	2	3	4
$h_r = 0.002$ m						
19×32:4	1×32:4	19×1:4	1075.8	1286.6	1856.5	1965.4
29×40:4	1×40:4	29×1:4	1059.5	1282.3	1826.9	1936.1
38×56:4	2×56:4	38×2:4	1050.0	1281.5	1815.6	1924.9
48×72:4	2×72:4	48×2:4	1046.2	1277.4	1808.9	1912.9
58×80:4	2×80:4	58×2:4	1045.1	1276.1	1805.5	1901.7
			(2,1)	(0,1)	(2,2)	(3,1)
$h_r = 0.004$ m						
19×32:4	1×32:8	19×1:8	1156.9	1251.7	1650.8	2072.7
29×40:4	1×40:8	29×1:8	1148.5	1240.7	1638.5	2034.2
38×56:4	2×56:8	38×2:8	1144.7	1231.7	1632.1	2015.3
48×72:4	2×72:8	48×2:8	1143.2	1224.9	1630.3	2005.0
58×80:4	2×80:8	58×2:8	1142.5	1222.8	1629.5	2001.5
			(0,1)	(2,1)	torsion motion	(2,2)
$h_r = 0.006$ m						
19×32:4	1×32:12	19×1:12	1155.4	1483.2	2132.8	2242.7
29×40:4	1×40:12	29×1:12	1146.5	1463.4	2117.6	2216.8
38×56:4	2×56:12	38×2:12	1141.6	1445.8	2104.0	2191.4
48×72:4	2×72:12	48×2:12	1139.8	1438.3	2099.1	2180.6
58×80:4	2×80:12	58×2:12	1138.8	1435.9	2097.2	2176.6
			(0,1)	(2,1)	(0,2)	(2,2)

Table 2. Convergence of natural frequencies (Hz) for a laminated stiffened shell with ring and string stiffeners (Example 2).

Example 3. Strictly speaking, to apply the theory in this paper, we must require the cross-section of the string to be a partial annulus (Figure 10, left). If the cross-section of the string is a rectangle, we can transform the rectangular cross-section of the string into a partial annulus (Figure 10, right). The following example, taken from [Stanley and Ganessan 1997], proves the method feasible. The shell has inside diameter $d = 0.2$ m, thickness $t = 0.002$ m and length $l = 0.4$ m; the strings have breadth $b_s = 0.004$ m and height $h_s = 0.004$ m. The numerical results and comparison are listed in Table 3.

Replacing the rectangular cross-section of the string by a partial annulus, as in the figure, increases the distance between the center of the cross-section and the coordinate origin. Hence, the results obtained by the present method are larger than those of the reference data [Stanley and Ganessan 1997]. It can be seen in Table 3 that the error increases with the mode order; this may be because the effect of distance on the natural frequencies is more prominent for higher modes.

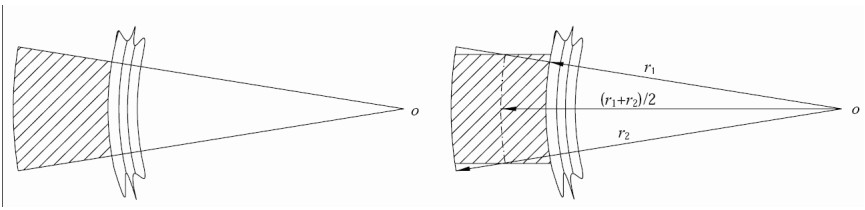

Figure 10. Cross-section of string (Example 3): left, partial annulus; right, switching from a rectangle to a partial annulus.

Mesh : layers		Mode number					
Shell	Strings	1	2	3	4	5	6
4 strings							
58×72:1	58×2:2	915.8 (4,1)	947.6 (3,1)	1227.9 (5,1)	1446.3 (2,1)	1563.5 (4,2)	1591.5 (5,2)
Experimental		914.1	944.9	1214	1432	1547	1571
Relative error		0.19%	0.50%	1.14%	1.00%	1.07%	1.30%
12 strings							
58×72:1	58×2:2	884.6 (4,1)	918.6 (3,1)	1179.5 (5,1)	1397.1 (2,1)	1511.2 (4,2)	1550.4 (5,2)
Experimental		881.7	913.6	1167	1380	1501	1529
Relative error		0.56%	0.55%	1.07%	1.24%	0.68%	1.40%

Table 3. Comparison of natural frequencies (Hz) for steel shell stiffened with strings and clamped at the edges (Example 3). "Experimental" refers to values from [Stanley and Ganessan 1997].

Example 4. Consider a 90° cylindrical panel with discontinuity in the thickness and one cutout (Figure 11). The material parameters for the external layer (ring stiffener) and the shell are the same as for the core layer and external layer, respectively, in Example 1. Two transversal cross-sections are shown; the method applies directly to the first, consisting only of partial annuli, but the idea of Example 3 is suitable here, allowing us to reduce the case of second cross-section to that of the first. The first six natural frequencies are given in Table 4.

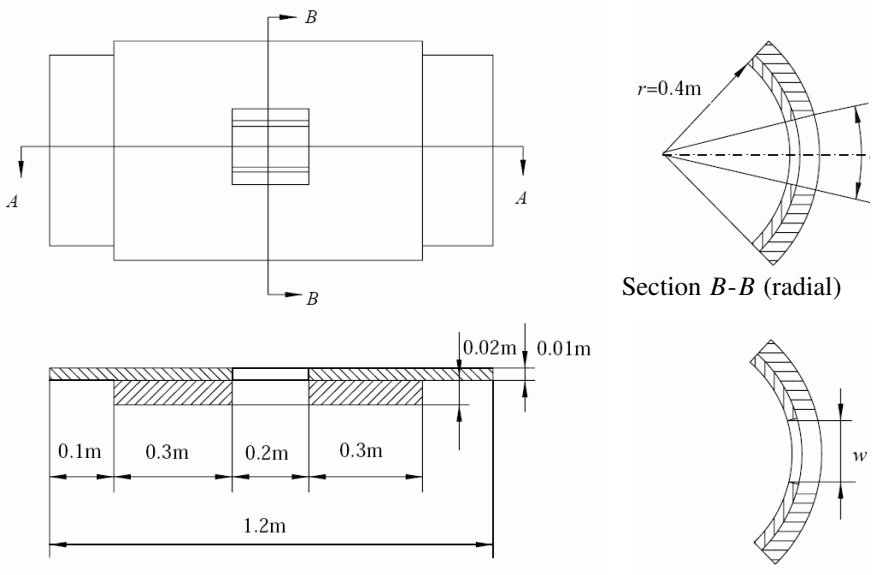

Figure 11. A 90° cylindrical panel with a cutout and discontinuity in thickness (Example 4).

Mesh : layers		Mode number					
Shell	Ring	1	2	3	4	5	6
4 strings							
12×12:1	10×12:2	1387.5	1630.7	2046.4	2071.0	2315.5	2375.1
24×24:1	20×24:2	1305.3	1519.7	1928.1	1943.4	2135.4	2192.7
36×36:1	30×36:2	1301.0	1515.5	1921.8	1936.1	2111.4	2175.3
48×48:1	40×48:2	1285.0	1497.6	1901.0	1909.1	2085.2	2154.5
60×60:1	50×60:2	1281.6	1489.7	1889.1	1904.1	2070.3	2139.7
72×72:1	50×60:2	1280.8	1488.8	1887.4	1902.2	2067.4	2136.2

Table 4. Natural frequencies (Hz) for cylindrical panel with discontinuity in thickness and clamped at all edges (Example 4).

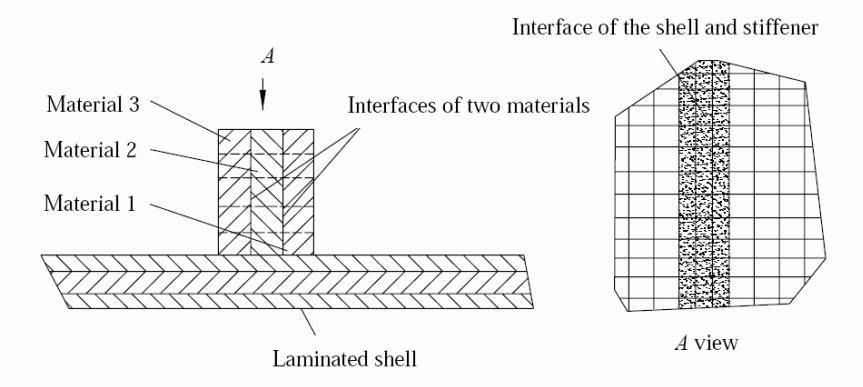

Figure 12. Type 2 stiffener.

In each of these examples, we have considered type 1 stiffeners and the material was the same over the cross-section of the stiffener. However, even if there are two or more materials in the cross-section of the stiffener, the method is also suitable without additional equations. This is because Equation (8) is used to handle the laminated shell that the material of every layer can be different.

If we are dealing with a type 2 stiffener (Figure 2), we can regard it as a layered shell (Figure 12), but there may be two or more materials in a layer. This situation is similar to the type 1 stiffener; the major difference is that we must pay attention to the interfaces of different materials when we discretize each layer of the stiffener. One element cannot include more than one material.

4. Conclusions

This paper introduces a general, novel mathematical model for the free vibration analysis of some stiffened cylindrical shells. In this model the shell and the stiffeners are discretized by the same quadrilateral element. The linear algebraic equations of the shell and stiffeners are established separately. The compatibility of displacements and stresses on the interface between the shell and the stiffeners is maintained. Numerical examples show that the current approach has excellent predictive ability. Some specific features of the model are:

(1) The three-dimensional free vibration problem of stiffened laminated shells is transformed into a two-dimensional one.

(2) The number of variables included in the global linear equation of the stiffened shell has no relationship with the number of layers of the shell and stiffeners. Hence, the number of variables is greatly reduced.

(3) Transverse shear deformation and rotational inertia are taken into account.

If a similar modified H-R mixed variational principle for piezoelectric materials and the corresponding discrete state-vector equation are established, the dynamic behavior of piezoelectric plates with piezoelectric patches [Lee and Saravanos 1997; Lin et al. 1996] and of cylindrical shells with piezoelectric rings or/and strings can be analyzed directly using the present approach.

Acknowledgment

The authors thank the reviewers for their valuable comments.

Appendix: Expressions for C^e, K^e, H^e in Equation (3)

We have $\boldsymbol{C}^e = \left(\iint \boldsymbol{N}^T \boldsymbol{N} \bar{r}\, |\boldsymbol{J}|\, d\xi\, d\eta\right)\boldsymbol{I}$, where $\boldsymbol{I}$ is the 6×6 unit matrix, $\bar{r}$ is the average of the inside radius r_i and the outside radius r_o of an element, and

$$\boldsymbol{J} = \begin{bmatrix} \displaystyle\sum_{i=1}^{4} \frac{\partial \boldsymbol{N}_i}{\partial \xi} x_i & \displaystyle\sum_{i=1}^{4} \frac{\partial \boldsymbol{N}_i}{\partial \xi} \theta_i \\ \displaystyle\sum_{i=1}^{4} \frac{\partial \boldsymbol{N}_i}{\partial \eta} x_i & \displaystyle\sum_{i=1}^{4} \frac{\partial \boldsymbol{N}_i}{\partial \eta} \theta_i \end{bmatrix}.$$

Further,

$$\boldsymbol{H}^e(r) = \left[u^e(r) \;\; v^e(r) \;\; w^e(r) \;\; \tau_{xr}^e(r) \;\; \tau_{\theta r}^e(r) \;\; \sigma_r^e(r)\right]^T$$

and

$$\boldsymbol{K}^e = \iint \begin{bmatrix} \boldsymbol{A}^e & \boldsymbol{B}^e \\ \boldsymbol{C}^e & \boldsymbol{D}^e \end{bmatrix} \bar{r}\, |\boldsymbol{J}|\, d\xi\, d\eta,$$

where, setting $\nu = \boldsymbol{N}^T \boldsymbol{N}$, $\lambda = \boldsymbol{N}^T \alpha \boldsymbol{N}$ and $\mu = \boldsymbol{N}^T \beta \boldsymbol{N}$, the matrix entries are

$$\boldsymbol{A}^e = \begin{bmatrix} 0 & 0 & -\lambda \\ 0 & r^{-1}\nu & -r^{-1}\mu \\ C_1\alpha\nu & C_5 r^{-1}\beta\nu & C_5 r^{-1}\nu \end{bmatrix},$$

$$\boldsymbol{B}^e = \begin{bmatrix} C_8\nu & 0 & 0 \\ 0 & C_9\nu & 0 \\ 0 & 0 & C_7\nu \end{bmatrix},$$

$$\boldsymbol{C}^e = \begin{bmatrix} -\rho\omega^2\nu + C_2\alpha\lambda + C_6 r^{-2}\beta\mu & C_3 r^{-1}\alpha\mu + C_6 r^{-1}\beta\lambda & C_3 r^{-1}\alpha\nu \\ C_3 r^{-1}\beta\lambda + C_6 r^{-1}\alpha\mu & -\rho\omega^2\nu + \alpha\lambda + C_6 r^{-2}\beta\mu & C_4 r^{-2}\beta\nu \\ C_3 r^{-1}\lambda & C_4 r^{-2}\mu & -\rho\omega^2\nu + C_4 r^{-2}\mu \end{bmatrix},$$

$$\boldsymbol{D}^e = \begin{bmatrix} -r^{-1}\nu & 0 & -C_1\lambda \\ 0 & -2r^{-1}\nu & -C_5 r^{-1}\mu \\ \alpha\nu & r^{-1}\beta\nu & -(C_5+1)\, r^{-1}\nu \end{bmatrix}.$$

References

[Al-Najafi and Warburton 1970] A. M. Al-Najafi and G. B. Warburton, "Free vibration of ring-stiffened cylindrical shells", *J. Sound Vib.* **13** (1970), 9–25.

[Gong and Lam 1998] S. W. Gong and K. Y. Lam, "Transient response of stiffened composite submersible hull subjected to underwater explosive shock", *Compos. Struct.* **41** (1998), 27–37.

[Johnston 1982] R. L. Johnston, *Numerical methods*, Wiley, New York, 1982.

[Kim and Lee 2002] Y. W. Kim and Y. S. Lee, "Transient analysis of ring-stiffened composite cylindrical shells with both edges clamped", *J. Sound Vib.* **252** (2002), 1–17.

[Lee and Saravanos 1997] H. J. Lee and D. A. Saravanos, "Generalized finite element formulation for smart multilayered thermal piezoelectric composite plates", *Int. J. Solids Struct.* **34**:26 (1997), 3355–3371.

[Liao and R. 1994] C. L. Liao and C. C. R., "Dynamic stability of stiffened laminated composite plates and shells subjected to in-plane pulsating forces", *J. Sound Vib.* **174**:3 (1994), 335–351.

[Lin et al. 1996] C. C. Lin, C. Y. Hsu, and H. N. Huang, "Finite element analysis on deflection control of plates with piezoelectric actuators", *Compos. Struct.* **35**:4 (1996), 423–433.

[Moler and Van Loan 1978] C. Moler and C. Van Loan, "Nineteen dubious ways to compute the exponential of a matrix", *SIAM Review* **20**:4 (1978), 801–836.

[Rikards et al. 2001] R. Rikards, A. Chate, and O. Ozolinsh, "Analysis for buckling and vibrations of composite stiffened shells and plates", *Compos. Struct.* **51**:4 (2001), 361–370.

[Sheng and Ye 2002a] H. Y. Sheng and J. Q. Ye, "A semi-analytical finite element for laminated composite plates", *Compos. Struct.* **57** (2002), 117–123.

[Sheng and Ye 2002b] H. Y. Sheng and J. Q. Ye, "A state space finite element for laminated composite plates", *Comput. Methods Appl. Mech. Eng.* **191**:37 (2002), 4259–4276.

[Sheng and Ye 2003] H. Y. Sheng and J. Q. Ye, "A three-dimensional state space finite element solution for laminated composite cylindrical shells", *Comput. Methods Appl. Mech. Eng.* **192**:22 (2003), 2441–2459.

[Sinha and Mukhopadhyay 1995] G. Sinha and M. Mukhopadhyay, "Transient dynamic response of arbitrary stiffened shells by the finite element method", *J. Vib. Acoustics* **117**:1 (1995), 11–16.

[Srinivasan and Krishnan 1989] R. S. Srinivasan and P. A. Krishnan, "Dynamic analysis of stiffened conical shell panels", *Comput. Struct* **33**:3 (1989), 831–837.

[Stanley and Ganessan 1997] A. J. Stanley and N. Ganessan, "Free vibration characteristics of stiffened cylindrical shells", *Comput. Struct.* **65**:1 (1997), 33–45.

[Steele and Kim 1992] C. R. Steele and Y. Y. Kim, "Modified mixed variational principle and the state-vector equation for elastic bodies and shells of revolution", *J. App. Mech.* (*ASME*) **59**:3 (1992), 587–595.

[Wang et al. 1997] M. Wang, S. Swaddiwudhipong, and J. Tian, "Ritz method for vibration analysis of cylindrical shells with ring stiffeners", *J. Engineer. Mech.* **123**:2 (1997), 134–142.

[Wilken and Soedel 1976] I. D. Wilken and W. Soedel, "The receptance method applied to ring-stiffened cylindrical shells: analysis of modal characteristics", *J. Sound Vib.* **44**:4 (1976), 563–576.

[Yang and Zhou 1995] B. Yang and J. Zhou, "Analysis of ring-stiffened cylindrical shells", *J. Appl. Mech.* **62**:4 (1995), 1005–1014.

[Zhao et al. 2002] X. Zhao, K. M. Liew, and T. Y. Ng, "Vibrations of rotating cross-ply laminated circular cylindrical shells with stringer and rings stiffeners", *Intl. J. Solids Struct.* **39**:2 (2002), 529–545.

[Zhong 2001] W. X. Zhong, "Combined method for the solution of asymmetric Riccati differential equation", *Comput. methods appl. mech. eng.* **191**:1 (2001), 93–102.

[Zhong and Zhu 1996] W. X. Zhong and J. P. Zhu, "Precise time integration for the matrix Riccati differential equation", *J. Numer. Methods Comput. Appl.* **17**:1 (1996), 26–35. In Chinese; translation in *Chinese J. Numer. Math. Appl.* **18**:4, (1996), 47–57. MR 97f:65047

[Zou and Tang 1995a] G. P. Zou and L. M. Tang, "A semi-analytical solution for laminated composite plates in Hamilton system", *Comput. Methods Appl. Mech. Eng.* **128**:3 (1995), 395–404.

[Zou and Tang 1995b] G. P. Zou and L. M. Tang, "A semi-analytical solution for thermal stress analysis of laminated composite plates in the Hamiltonian system", *Comput. Struct.* **55**:1 (1995), 113–118.

Received 24 Sep 2005. Revised 10 Dec 2005.

GUANGHUI QING: qingluke@126.com
Aeronautical Mechanics and Avionics Engineering College, Civil Aviation University of China, Tianjin 300300, People's Republic of China

ZHENYU FENG: *Aeronautical Mechanics and Avionics Engineering College, Civil Aviation University of China, Tianjin 300300, People's Republic of China*

YANHONG LIU: *Aeronautical Mechanics and Avionics Engineering College, Civil Aviation University of China, Tianjin 300300, People's Republic of China*

JIAUJUN QIU: *Department of Mechanics and Engineering Measurement, School of Mechanical Engineering, Tianjin University, Tianjin 300072, People's Republic of China*